Generation of below-threshold even harmonics by a stretched H_{2}^{+} molecular ion in intense linearly and circularly polarized laser fields

K. Nasiri Avanaki, Dmitry A. Telnov, H. Z. Jooya, and Shih-I Chu

Phys. Rev. A **92**, 063811 — Published 8 December 2015

DOI: 10.1103/PhysRevA.92.063811

Generation of below-threshold even harmonics by stretched H_2^+ molecular ion in intense linearly and circularly polarized laser fields

K. Nasiri Avanaki,[1,*] Dmitry A. Telnov,[2,†] H. Z. Jooya,[1,‡] and Shih-I Chu[1,3,§]

[1] *Department of Chemistry, University of Kansas, Lawrence, Kansas 66045*
[2] *Department of Physics, St. Petersburg State University, 7/9 Universitetskaya nab., St. Petersburg 199034, Russia*
[3] *Center for Quantum Science and Engineering, Department of Physics, National Taiwan University, Taipei 10617, Taiwan*

(Dated: November 16, 2015)

We explore the mechanism of below-threshold even-harmonic generation of the H_2^+ molecular ion subject to intense near-infrared linearly and circularly polarized laser fields. The task is accomplished by accurate treatment of the time-dependent Schrödinger equation in prolate spheroidal coordinates within the generalized pseudospectral formalism. Even harmonics are detected in the harmonic spectra of stretched molecules, mostly with the internuclear separations of 5 to 9 a.u. Consecutive dynamic localization of the electron density near each of the nuclei is responsible for the broken inversion symmetry, which in turn leads to emission of low-order even harmonics. An intuitive picture of the process is provided by the analysis of the time evolution of the electron density and time-frequency spectra of the dipole acceleration. A clear theoretical explanation of the phenomenon is given within the Floquet formalism.

PACS numbers: 33.80.-b,42.65.Ky,42.50.Hz

I. INTRODUCTION

Recently more attention has been paid to generation of the below-threshold harmonics (BTH) as a potential approach to produce novel light sources in the vacuum-ultraviolet (VUV) band due to the higher conversion efficiency [1]. Several theoretical and experimental studies [2–4], particularly in elliptically polarized field [5], for BTH have been performed. For a certain order of BTH, abnormal ellipticity dependence of the harmonic yield was observed [6]. However, the mechanism of the BTH generation is still not understood very well and remains an open question. Even though the traditional three-step model [7] of high harmonic generation cannot be applied directly to this energy region, one can still use it as a qualitative tool to understand the harmonic generation (HG) process in linearly polarized laser fields [4, 8–10]. According to the generalized semiclassical model [8], the atomic (molecular) core potential plays an important role during the excursion of the electron in the laser field and makes it possible for the returning electron to have the total energy less than zero thus leading to emission of below-threshold harmonics. It was found that only the long trajectories in the tunneling ionization regime can contribute to BTH through this mechanism. For elliptical and circular polarization of the driving field, the recollision is not intuitive. The transverse component of the laser field tilts the trajectory of the electron and prevents it from recombining with the parent nucleus. However, in two-center systems such as diatomic molecules, recombination can still occur on the other nucleus [11]. Another contribution to generation of BTH comes from the multiphoton mechanism [8]. The phases of these two contributions have different dependence on the intensity of the driving laser field; their interference results in prominent steps in the intensity-dependent yield of these harmonics [8]. Recent calculations by Xiong *et al.* [12] reveal that, besides the quantum path interference mechanism, resonance effects have a crucial impact on the BTH generation. Thus it appears that several mechanisms beyond the perturbation theory can be involved in the HG process below the ionization threshold, and the HG spectra in this energy region cannot be fully explained using only one mechanism.

In our previous work [13], we reported an observation of weak yet well pronounced even harmonics in the below-threshold region of the HG spectra in stretched H_2^+ molecules. To the best of our knowledge, the mechanism of generation of even harmonics in this quantum system has not been fully investigated. Because of the fundamental symmetry, which includes the inversion symmetry of the media and the half-wave symmetry of the driving field, generation of even harmonics is forbidden. In atoms, due to the spatial inversion symmetry of the electron-nucleus interaction, only odd harmonics are present in the HG spectra [14]. Strictly speaking, if the driving field represents a pulse and not a continuous wave, the half-wave symmetry is broken, and generation of even harmonics is possible [15]. However, this effect is negligible for long enough pulses like those containing 20 optical cycles. The same argument is valid for homonuclear diatomic molecules. Only for the gas of *oriented heteronuclear* diatomic molecules one can expect to see both odd and even harmonics in the HG spectra [16].

* nasiri@ku.edu
† d.telnov@spbu.ru
‡ jooya@ku.edu
§ sichu@ku.edu

The HG spectra of the stretched ($R = 7$ a.u.) homonuclear diatomic molecular ion H_2^+ in circularly polarized laser fields showed a comb of well-resolved odd and even harmonics, particularly in below-threshold region of the spectra [13]. We explained this unexpected pattern in the HG spectra by the effect of a dynamical rupture of symmetry (DRS) [17]. In the unperturbed H_2^+, the electron density is symmetrically distributed over the two nuclei. Under the influence of the external field, the electron density becomes sequentially localized over one of the nuclei, and repeatedly bounces back and forth from one nucleus onto another. During the localization time over one of the nuclei, the electron experiences a non-symmetric potential, which is the sum of the symmetric atomic potential of the near nucleus plus the tail of the potential of the far nucleus; this dynamic breaking of the inversion symmetry causes the emission of even harmonics. In the stretched configuration, the two lowest electronic states of H_2^+, $1\sigma_g$ and $1\sigma_u$, become nearly degenerate as the internuclear separation R increases. The electric dipole coupling of these two states at large R grows linearly with R and becomes very significant. This phenomenon takes place only in the odd-charged molecular-ion systems and it is known as the "charge resonance" (CR) effect [18]. In H_2^+ subject to laser fields, DRS is also enhanced by existence of the CR effect. In the present paper, we elaborate on the dynamically broken inversion symmetry in stretched H_2^+ molecules using various laser wavelengths and internuclear distances in the calculations. Although the phenomenon is not specific for non-zero ellipticity only, it becomes more pronounced when the ellipticity parameter is large enough, particularly in the case of the circular polarization of the driving field.

II. THEORETICAL AND COMPUTATIONAL METHOD

In this paper we analyze the elliptical field and internuclear separation effects in harmonic generation of diatomic molecules, using the simplest diatomic molecule, hydrogen molecular ion H_2^+. We solve the time-dependent Schrödinger equation(atomic units $\hbar = m = e = 1$ are used unless stated otherwise):

$$i\frac{\partial}{\partial t}\Psi(\boldsymbol{r},t) = H(t)\Psi(\boldsymbol{r},t) \tag{1}$$

where $H(t)$ is the full Hamiltonian, including the time-dependent interaction with the laser field

$$H(t) = -\frac{1}{2}\nabla^2 + U(\boldsymbol{r}) + V_{\rm ext}(\boldsymbol{r},t). \tag{2}$$

In Eq. (2), the first two terms are the unperturbed electronic Hamiltonian H_0 and $V_{\rm ext}(\boldsymbol{r},t)$ is the interaction with the laser field. Assuming the elliptically polarized (EP) laser field is in the $x-z$ plane, we solve the time-dependent Schrödinger equation (TDSE) in the prolate spheroidal coordinates ξ, η, and φ, which are related to Cartesian coordinates x, y, and z as

$$x = a\sqrt{(\xi^2-1)(1-\eta^2)}\cos\varphi, \tag{3}$$
$$y = a\sqrt{(\xi^2-1)(1-\eta^2)}\sin\varphi, \tag{4}$$
$$z = a\xi\eta. \tag{5}$$

Here $a = R/2$ is a half internuclear distance. Using the prolate spheroidal coordinates, the interaction with the laser field $V_{\rm ext}(\boldsymbol{r},t)$ can be written as follows:

$$V_{\rm ext}(\boldsymbol{r},t) = \frac{aF(t)}{\sqrt{1+\epsilon^2}}\Big[\xi\eta\sin(\omega_0 t) + \epsilon\sqrt{(\xi^2-1)(1-\eta^2)}\cos\varphi\cos(\omega_0 t)\Big], \tag{6}$$

where ω_0 is the carrier frequency and ϵ is the ellipticity parameter; $\epsilon = 0$ corresponds to the linear polarization of the laser field along the z (molecular) axis while $\epsilon = 1$ describes the circular polarization in the $x-z$ plane. For the time-dependent pulse envelope $F(t)$, we use a sine-squared shape:

$$F(t) = F_0\sin^2\left(\frac{\pi t}{NT}\right) \tag{7}$$

Here F_0 is the peak field amplitude, $T = 2\pi/\omega_0$ is the duration of one optical cycle, and N is the number of optical cycles in the pulse. We apply the time-dependent generalized pseudospectral method (TDGPS) [19, 20] to discretize and propagate the time-dependent wave function using the second-order split-operator method in the energy representation:

$$\Psi(\boldsymbol{r},t+\Delta t) = \exp\left[-i\frac{\Delta t}{2}H_0(\boldsymbol{r})\right] \times \exp\left[-i\Delta t V(\xi,\eta,t+\frac{\Delta t}{2}\right] \times \exp\left[-i\frac{\Delta t}{2}H_0(\boldsymbol{r})\right]\Psi(\boldsymbol{r},t) + O(\Delta t^3). \tag{8}$$

Detailed numerical procedures can be found in Ref. [19, 21]. Adopting proper numerical parameters such as the number of grid points, the box size, and absorber position, we reproduce the ground state of H_2^+ with the machine accuracy. To obtain the HG spectra for the laser field parameters and internuclear separations used in the calculations, we set the grid size (for the ξ, η, and φ coordinates, respectively) to $180\times58\times48$ in the circularly polarized (CP) field and to $224\times32\times16$ in the linearly polarized (LP) field. We use 4096 time steps per optical cycle (81920 steps for the total pulse of 20 optical cycles) in the time propagation process. All spatial and temporal parameters have been varied to make sure all the harmonic spectra are fully converged. Choosing the linear dimension of the box at 60 a.u., we guarantee the accurate description of all the important physics for the laser field parameters used in the calculations. In order

to prevent artificial reflections of the wave packet from the grid boundary, we place an absorber in the layer between 40 and 60 a.u.

Once the time-dependent wave function is available, we can proceed to calculate the spectra of the emitted harmonic radiation. In order to calculate the HG spectra, we employ the general semiclassical approach, substituting the classical quantities with the corresponding quantum expectation values. The spectral density of the harmonic radiation energy is given by either the length form,

$$S(\omega) = \frac{2\omega^4}{3\pi c^3}|\boldsymbol{D}_\omega|^2, \tag{9}$$

or acceleration form,

$$S(\omega) = \frac{2}{3\pi c^3}|\boldsymbol{A}_\omega|^2. \tag{10}$$

Here $\boldsymbol{D}_\omega$ and $\boldsymbol{A}_\omega$ are the Fourier transforms of the time-dependent dipole moment and dipole acceleration, respectively. The length and acceleration forms provide almost identical results for HG spectra, indicating good quality of our wave functions.

The dynamics of the HG process can be explored in more detail using the time-frequency analysis of the dipole acceleration by means of the wavelet transformation [22]:

$$\tilde{\boldsymbol{A}}_{\rm w}(\omega, t) = \sqrt{\omega}\int_{-\infty}^{\infty} dt' W[\omega(t'-t)]\boldsymbol{A}(t'). \tag{11}$$

For our purposes, the natural choice of the mother wavelet $W(x)$ is the Morlet wavelet:

$$W(x) = \exp(ix)\exp\left(-\frac{x^2}{2\tau^2}\right), \tag{12}$$

so Eq. (11) represents a type of short-time Fourier transform. For the window width parameter τ, we use the value $\tau = 15$, previously tested and adopted for the time-frequency analysis of HG signals [23, 24]. The quantity $\tilde{\boldsymbol{A}}_{\rm w}(\omega, t)$ provides the time profile of the harmonic with the frequency ω and thus reveals what parts of the laser pulse on the time scale are mainly responsible for generation of the harmonic signals with specific frequencies.

III. RESULTS AND DISCUSSION

We have performed the calculations of the HG spectra emitted by a stretched H_2^+ molecule initially in the $1\sigma_g$ electronic state. We used both the LP and CP laser fields with three different carrier wavelengths in the near-infrared range (640, 800, and 1064 nm). In all cases, the laser pulse has a sine-squared envelope and total duration of 20 optical cycles. Since HG is a highly nonlinear process, the key role is played not by the time average of the energy flux (intensity) but by the peak value of the electric field strength. For the same peak value of the electric field F_0, the intensity of the LP field ($I = cF_0^2/(8\pi)$, c being the speed of light) is twice as small as that of the CP field ($I = cF_0^2/(4\pi)$). Thus it makes more sense to compare the HG spectra in the LP and CP laser fields at *different* intensities, with the intensity of the CP field two times larger than that of the LP field.

Fig. 1 shows the HG spectra of the H_2^+ molecular ion initially in the $1\sigma_g$ state with the internuclear separation $R = 7$ a.u. for both CP and LP fields and all three carrier wavelengths. The peak intensity is 1×10^{14} W/cm^2 for the LP field and 2×10^{14} W/cm^2 for the CP field. According to the well-known atomic recollision model [7], in the case of the LP field with the intensity I, the cutoff in the HG spectrum is located around the energy $I_P + 3.17U_P$ where U_P is the ponderomotive potential ($U_P = I/4\omega_0^2$) and I_P is the ionization energy of the initial state. For H_2^+ in the $1\sigma_g$ state at $R = 7$ a.u., the vertical ionization energy is 0.648 a.u. At $I = 1 \times 10^{14}$ W/cm^2, the harmonic orders corresponding to the cutoff are equal to 15, 23, and 43 for the wavelengths 640, 800, and 1064 nm, respectively. The below-threshold region in the HG spectrum is defined as that with the photon energies less or equal to I_P. Thus the below-threshold harmonics are those with the orders less or equal to 9, 11, and 15 for the wavelengths 640, 800, and 1064 nm, respectively.

Normally one expects to see only odd harmonics in the HG spectra. However, the spectra in Fig. 1 also exhibit weak even harmonics in the below-threshold region. These even harmonic peaks appear more distinct in the case of CP field and become larger as the carrier wavelength increases. They become less pronounced in the above-threshold region.

We have further studied generation of even harmonics at different internuclear separations. Fig. 2 shows the HG spectra of the H_2^+ molecular ion under LP and CP fields with the carrier wavelength 1064 nm at the internuclear separations 3 to 6 a.u., for the initial $1\sigma_g$ state. The peak intensity in this set of calculations is 1×10^{14} W/cm^2 for the LP field and 2×10^{14} W/cm^2 for the CP field. When the internuclear distance R increases, the vertical ionization potential decreases, so does the energy difference between the $1\sigma_g$ and $1\sigma_u$ states. At the smallest $R = 3$ a.u. used in the calculations (Figs. 2a and 2b), there are no visible even harmonics in the spectra; however, one can notice the enhanced 5th harmonic and an extra peak at the harmonic order 5.28. The 3rd, 7th, and 9th harmonics are also split in two peaks each. We attribute this behavior of the HG spectra to the 5-photon resonance between the ground $1\sigma_g$ state and the first excited state $1\sigma_u$ state. For larger R, the HG spectra in the below-threshold region appear more complex. At $R = 5$ a.u. (Figs. 2e and 2f), the even harmonics are as strong as the odd harmonics and have a double-peak structure. At $R = 6$ a.u. (Figs. 2g and 2h), they still exhibit a double-peak structure but become weaker. As we will discuss below, enhanced generation of even harmonics and their double-peak structure are related to strong coupling between the $1\sigma_g$ and $1\sigma_u$ states, particularly in the vicinity

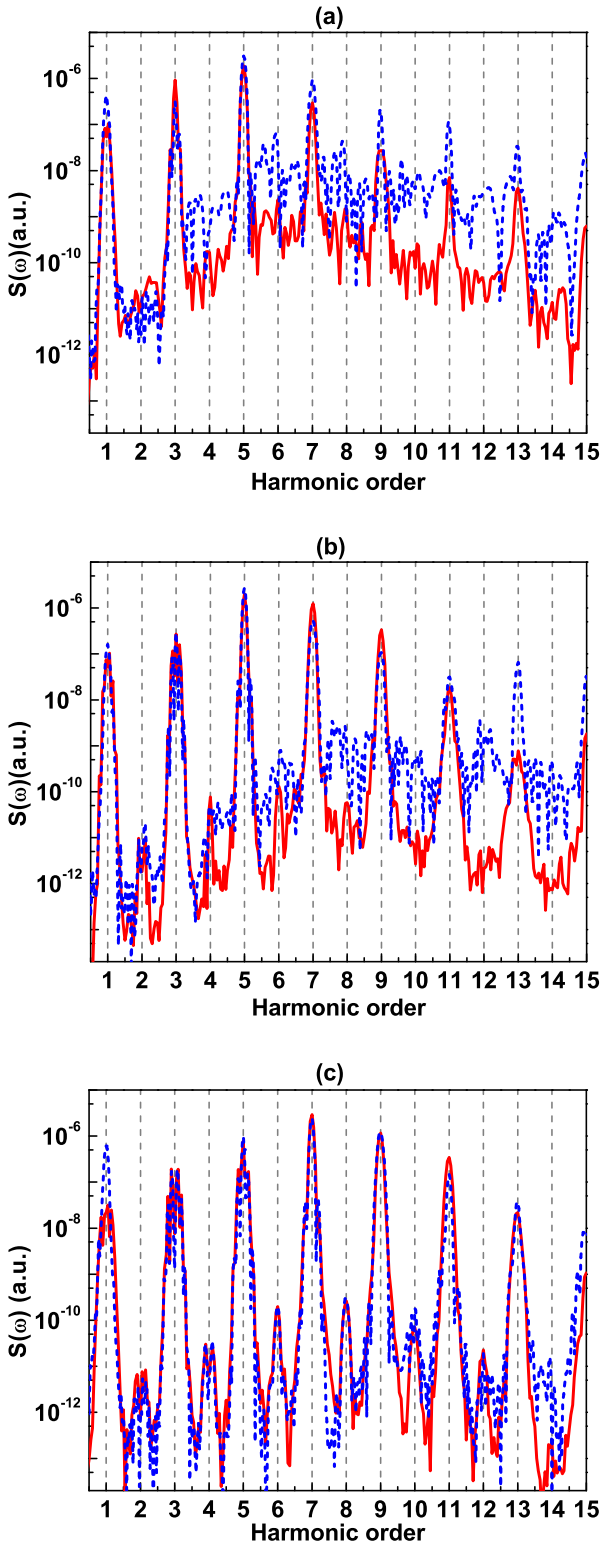

FIG. 1. (Color online) HG spectra of H_2^+ molecular ion initially in $1\sigma_g$ state at internuclear separation $R = 7$ a.u. Shown are the results for LP field with the peak intensity of 1×10^{14} W/cm^2 (dashed blue line) and CP field with the peak intensity of 2×10^{14} W/cm^2 (solid red line): panel (a), the carrier wavelength 640 nm; panel (b), the carrier wavelength 800 nm; panel (c), the carrier wavelength 1064 nm.

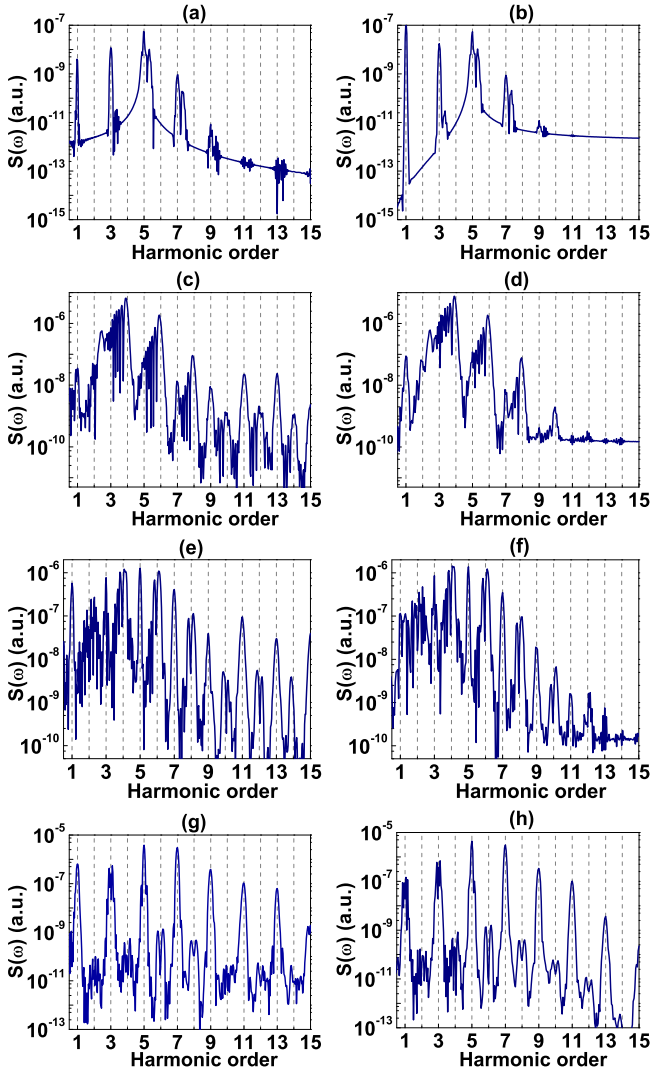

FIG. 2. (Color online) HG spectra of H_2^+ molecular ion initially in $1\sigma_g$ state at different internuclear separations: $R = 3$ a.u. [panels (a) and (b)], $R = 4$ a.u. [panels (c) and (d)], $R = 5$ a.u. [panels (e) and (f)], and $R = 6$ a.u. [panels (g) and (h)]. Left panels represent LP field with the peak intensity 1×10^{14} W/cm^2, right panels – CP field with the peak intensity 2×10^{14} W/cm^2. The carrier wavelength is 1064 nm.

of the one-photon resonance at $R = 5$ a.u.

To illustrate the dynamics of HG in both LP and CP fields, we have performed the time-frequency analysis of the dipole acceleration according to Eq. (11). Fig. 3 shows an absolute value of the wavelet transform (11) for the z-projection of the dipole acceleration. The results are presented for the carrier wavelength 1064 nm and internuclear distances $R = 3$ a.u. and $R = 5$ a.u. The peak intensity of the laser pulse is 1×10^{14} W/cm^2 for LP field and 2×10^{14} W/cm^2 for CP field. As one can see, for the same internuclear separation, the time-frequency spectra for the LP and CP fields are very similar. As expected, the main contribution to the harmonic signal

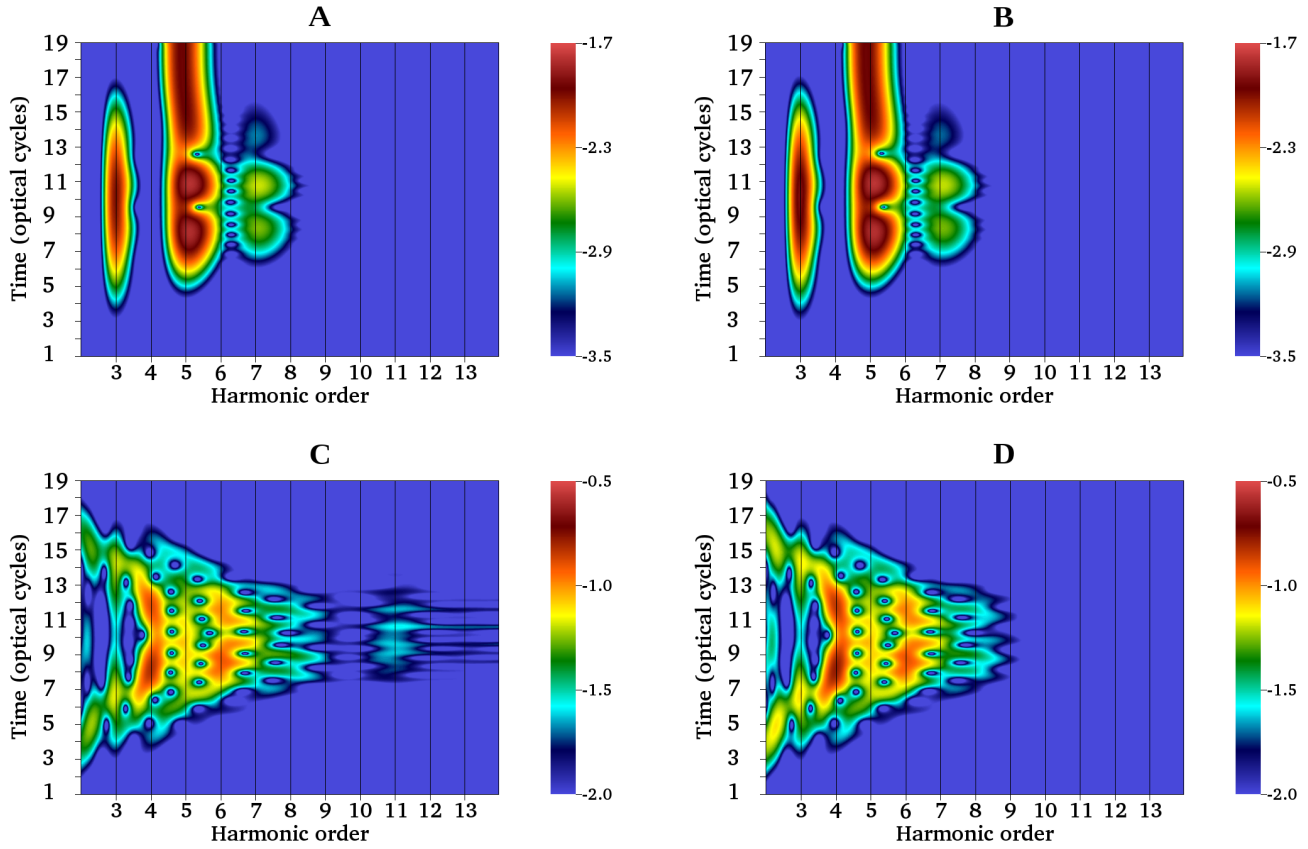

FIG. 3. (Color online) Wavelet time-frequency spectra (absolute value) of the dipole acceleration along the molecular axis (z direction) in stretched H_2^+ molecules subject to laser pulses with the carrier wavelength 1064 nm. Panel A: LP field at $I = 1\times10^{14}$ W/cm^2 and $R = 3$ a.u. Panel B: CP field at $I = 2\times10^{14}$ W/cm^2 and $R = 3$ a.u. Panel C: LP field at $I = 1\times10^{14}$ W/cm^2 and $R = 5$ a.u. Panel D: CP field at $I = 2\times10^{14}$ W/cm^2 and $R = 5$ a.u. The color scale is logarithmic.

comes from the central part of the laser pulse where the field is the strongest. At $R = 3$ a.u. one can see a strong line close to the harmonic order 5, which does not vanish even at the end of the pulse. This line is due to the 5-photon resonance between the ground $1\sigma_g$ and first excited $1\sigma_u$ states. Before the laser pulse, the $1\sigma_u$ state is not populated. However, because of the resonance, it gains a significant population when the laser field is switched on. This population remains in the $1\sigma_u$ state until the end of the pulse giving rise to emission of radiation. While only odd harmonic lines are present in the time-frequency spectra at $R = 3$ a.u., both odd and even lines show up at $R = 5$ a.u. Moreover, the even 4th and 6th harmonics appear the most intense among all below-threshold harmonics.

Generation of even harmonics indicates that the half-wave symmetry may be broken in this process. The half-wave symmetry of the time-periodic external field is expressed by the equation

$$V_{\rm ext}(-\boldsymbol{r}, t + T/2) = V_{\rm ext}(\boldsymbol{r}, t) \qquad (13)$$

where T is the period. It results in a similar relation for the electron density of the quantum system in the field,

$$\rho(-\boldsymbol{r}, t + T/2) = \rho(\boldsymbol{r}, t), \qquad (14)$$

provided the initial field-free state possesses the inversion symmetry. Strictly speaking, Eq. (13) holds only for the continuous-wave field and is not valid for the pulse with the time-dependent envelope. However, for a long enough laser pulse such as that containing 20 optical cycles, Eq. (14) is generally satisfied with a high accuracy, and even harmonics do not show up in the HG spectra. An exception is made by the case when the initial state does not possess the inversion symmetry or *may lose the symmetry* under the influence of the external field when the latter is switched on.

To illustrate the possible half-wave symmetry breaking in the laser field, we have calculated the time-dependent probability to find the electron in the left half-space ($z < 0$) and right half-space ($z > 0$). The plane $z = 0$ is the symmetry plane for H_2^+ since the nuclei are located on the z-axis at the points $z = -R/2$ and $z = R/2$. Figure 4 shows the results for both LP and CP fields in the two cases where the HG spectra differ qualitatively, $R = 3$ a.u. and $R = 5$ a.u. As one can see, at $R = 3$ a.u.

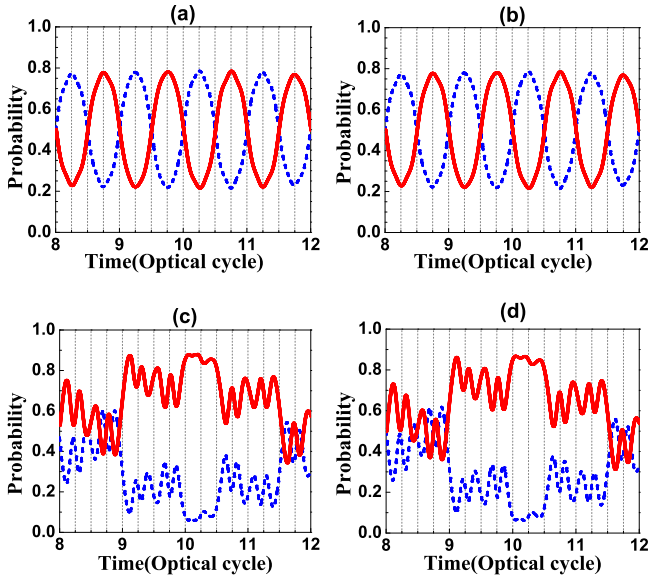

FIG. 4. (Color online) Probability to find the electron in the left half-space ($z < 0$) (dashed blue line) and right half-space ($z > 0$) (solid red line) as a function of time in the central part of the laser pulse (8 to 12 optical cycles). Shown are the cases of LP field at $I = 1 \times 10^{14}$ W/cm^2 [panels (a) and (c)] and CP field at $I = 2 \times 10^{14}$ W/cm^2 [panels (b) and (d)]. The internuclear separation R is equal to 3 a.u. [panels (a) and (b)] and 5 a.u. [panels (c) and (d)].

the probabilities to find the electron in the left half-space and the right half-space (that is, in the vicinity of the first nucleus and the second nucleus) correspond to the half-wave symmetry equation (14): the electron density oscillates between the two nuclei in phase with the laser field. The picture is totally different at $R = 5$ a.u. Here the half-wave symmetry is broken in the central part of the laser pulse where the field reaches its peak intensity. During this period of time (optical cycles 9 to 11), the electron predominantly resides in the vicinity of only one nucleus.

The observed features of the HG spectra can be explained with the help of the following approximate theoretical description, based on the analysis of HG in quantum systems described within the Floquet formalism [25–27]. In the central part of the laser pulse, where the pulse envelope is close to its maximum, the laser field can be approximated as a monochromatic field with the intensity equal to the peak intensity of the pulse. Then the wave function of the electron can be represented as a Floquet wave function. However, strong coupling between the $1\sigma_g$ and $1\sigma_u$ states due to the CR effect and possible tuning into a resonance at the particular carrier frequency and internuclear separation make the picture more complicated. Namely, the electron wave function is represented by a linear combination of *two* Floquet states, originating from the unperturbed $1\sigma_g$ and $1\sigma_u$ states, respectively, and having opposite parities with respect to the half-wave inversion (inversion of the coordinates and shift in time by a half optical cycle):

$$\Psi(\boldsymbol{r},t) = a_1 \exp(-i\varepsilon_1 t)\sum_n \psi_{1,n}(\boldsymbol{r})\exp(-in\omega t) + a_2 \exp(-i\varepsilon_2 t)\sum_n \psi_{2,n}(\boldsymbol{r})\exp(-in\omega t). \quad (15)$$

Here ε_1, $\psi_{1,n}(\boldsymbol{r})$ and ε_2, $\psi_{2,n}(\boldsymbol{r})$ are the quasienergies and Fourier components of the Floquet states 1 and 2, respectively. The weights a_1 and a_2 of these two Floquet states in the linear combination can be comparable to each other, particularly under the resonance conditions.

The time-dependent dipole moment is calculated as an expectation value of the electron radius-vector $\boldsymbol{r}$:

$$\boldsymbol{D}(t) = \int d^3r\ \boldsymbol{r}\rho(\boldsymbol{r},t) \quad (16)$$

and can be expanded in a sum of three contributions:

$$\boldsymbol{D}(t) = \boldsymbol{D}_{11}(t) + \boldsymbol{D}_{22}(t) + \boldsymbol{D}_{12}(t), \quad (17)$$

which result from the corresponding expansion of the electron density:

$$\rho(\boldsymbol{r},t) = \rho_{11}(\boldsymbol{r},t) + \rho_{22}(\boldsymbol{r},t) + \rho_{12}(\boldsymbol{r},t), \quad (18)$$

$$\rho_{11}(\boldsymbol{r},t) = \sum_{n,n'} \psi_{1,n}(\boldsymbol{r})\psi^*_{1,n'}(\boldsymbol{r})\exp[i(n'-n)\omega t], \quad (19)$$

$$\rho_{22}(\boldsymbol{r},t) = \sum_{n,n'} \psi_{2,n}(\boldsymbol{r})\psi^*_{2,n'}(\boldsymbol{r})\exp[i(n'-n)\omega t], \quad (20)$$

$$\rho_{12}(\boldsymbol{r},t) = 2\mathrm{Re}\Big\{\exp[-i(\varepsilon_1-\varepsilon_2)t] \times \sum_{n,n'} \psi_{1,n}(\boldsymbol{r})\psi^*_{2,n'}(\boldsymbol{r})\exp[i(n'-n)\omega t]\Big\}. \quad (21)$$

The Floquet states 1 and 2 evolve from the symmetric ($1\sigma_g$) and antisymmetric ($1\sigma_u$) unperturbed states of H_2^+, respectively, upon adiabatically slow switch on the laser field. That is why their Fourier components satisfy the following symmetry with respect to the inversion of the coordinates:

$$\psi_{1,n}(-\boldsymbol{r}) = (-1)^n\psi_{1,n}(\boldsymbol{r}), \quad (22)$$

$$\psi_{2,n}(-\boldsymbol{r}) = (-1)^{n+1}\psi_{2,n}(\boldsymbol{r}). \quad (23)$$

Consequently, both $\rho_{11}(\boldsymbol{r},t)$ and $\rho_{22}(\boldsymbol{r},t)$ possess the half-wave inversion symmetry:

$$\rho_{11}(-\boldsymbol{r},t+\frac{\pi}{\omega}) = \rho_{11}(\boldsymbol{r},t), \quad (24)$$

$$\rho_{22}(-\boldsymbol{r},t+\frac{\pi}{\omega}) = \rho_{22}(\boldsymbol{r},t). \quad (25)$$

Then it follows from Eqs. (16)–(20) that

$$\boldsymbol{D}_{11}(t+\frac{\pi}{\omega}) = -\boldsymbol{D}_{11}(t), \quad (26)$$

$$\boldsymbol{D}_{22}(t+\frac{\pi}{\omega}) = -\boldsymbol{D}_{22}(t). \quad (27)$$

According to Eqs. (19) and (20), $\boldsymbol{D}_{11}(t)$ and $\boldsymbol{D}_{22}(t)$ can be expanded in the Fourier series containing integer multiples of the fundamental frequency ω. Equations (26)

and (27) mean that only odd Fourier components are present in these series expansions, hence only odd harmonics may result from $\boldsymbol{D}_{11}(t)$ and $\boldsymbol{D}_{22}(t)$ contributions to the total dipole moment. This is not the case for $\boldsymbol{D}_{12}(t)$. It follows from Eq. (21) that the Fourier series for $\boldsymbol{D}_{12}(t)$ contains the frequencies $n\omega \pm \Delta\varepsilon$ where n is integer and $\Delta\varepsilon = \varepsilon_1 - \varepsilon_2$:

$$\boldsymbol{D}_{12}(t) = \sum_n \Big\{ \exp[i(n\omega - \Delta\varepsilon)t] \sum_{n'} \boldsymbol{d}_{n',n'+n} + \exp[i(n\omega + \Delta\varepsilon)t] \sum_{n'} \boldsymbol{d}^*_{n',n'-n} \Big\}. \tag{28}$$

In Eq. (28), the notation $\boldsymbol{d}_{n,n'}$ is used for the following dipole matrix element:

$$\boldsymbol{d}_{n,n'} = \int d^3r \; \boldsymbol{r} \psi_{1,n}(\boldsymbol{r}) \psi^*_{2,n'}(\boldsymbol{r}). \tag{29}$$

From the wave function symmetry properties (22) and (23) one can obtain that

$$\boldsymbol{d}_{n',n'\pm n} = (-1)^n \boldsymbol{d}_{n',n'\pm n}. \tag{30}$$

Then only even n numbers, $n = 2N$, contribute to the Fourier series of $\boldsymbol{D}_{12}(t)$, and Eq. (28) is recast in the following form:

$$\boldsymbol{D}_{12}(t) = \sum_N \Big\{ \exp[i(2N\omega - \Delta\varepsilon)t] \sum_{n'} \boldsymbol{d}_{n',n'+2N} + \exp[i(2N\omega + \Delta\varepsilon)t] \sum_{n'} \boldsymbol{d}^*_{n',n'-2N} \Big\}. \tag{31}$$

Generally, the radiation emitted due to the $\boldsymbol{D}_{12}(t)$ term is not restricted to integer multiples of the fundamental frequency ω and depends on the quasienergy difference $\Delta\varepsilon$. This conclusion is in full agreement with the general Floquet analysis of HG [25, 27] and previosuly established selection rules [26]. We also note that the Floquet theory was successfully used in the past to treat atoms and molecules in laser fields. A complex quasienergy approach in combination with complex scaling of the electronic coordinates provides an accurate description of ionization and HG processes in one-color [28, 29] and two-color [30–32] laser fields. The shape of the laser pulse can be taken into account, too [33, 34]. More references on the Floquet method can be found in the review paper [35].

For the system under consideration, two limiting cases deserve a special attention, however. The first case is when the quasienergies ε_1 and ε_2 are very close to each other, that is the $1\sigma_g$ and $1\sigma_u$ states are almost degenerate. This happens at large internuclear separations. For example, at $R = 7$ a.u. the unperturbed energies of the $1\sigma_g$ and $1\sigma_u$ states are equal to -0.648 and -0.639 a.u., respectively, and their difference is much smaller than the photon energy (the latter is equal to 0.0428 a.u. for the wavelength 1064 nm). In this case, one can neglect $\Delta\varepsilon$ in Eq. (31), and the $\boldsymbol{D}_{12}(t)$ contribution to the total dipole moment will produce *even* harmonics in the HG spectra. This is what we see in Figs. 1 and 2 at $R = 6$ a.u. and $R = 7$ a.u. If small $\Delta\varepsilon$ is taken into account, then the even harmonics exhibit a double-peak structure. The system is far from the one-photon resonance, and only the CR effect is responsible for the population of the second Floquet state. As a result, the even harmonics are relatively weak, compared with the odd harmonics. In Ref. [27], a 1D model of H_2^+ was used, and even harmonics in the HG spectra were found when the initial state was prepared as a superposition of the $1\sigma_g$ and $1\sigma_u$ states with the broken inversion symmetry. We note that in our calculations the initial state is always $1\sigma_g$, and the inversion symmetry is *not* broken at the beginning of the laser pulse. The dynamic rupture of the symmetry is caused by the laser field, which is actually not monochromatic, and the half-wave symmetry equation (13) does not apply on the leading and trailing edges of the laser pulse.

The second case is when the quasienergy difference $\Delta\varepsilon$ is close to an odd integer multiple of ω, and the system is in the vicinity of a resonance between $1\sigma_g$ and $1\sigma_u$ states. In this case, the second Floquet state is significantly populated, and the HG spectra exhibit very strong peaks located outside traditional odd integer multiples of the fundamental frequency. It can be a double-peak structure of odd harmonics, as seen in the case of the narrow five-photon resonance at $R = 3$ a.u. (see Figs. 2a and 2b), or very strong peaks close to even harmonics in the case of a broader one-photon resonance at $R = 5$ a.u. (Figs. 2e and 2f). We note that the quasienergies, and hence the detuning of the resonance, depend on the intensity of the field. That is why the pattern in the HG spectra for the same laser wavelength and internuclear distance of H_2^+ may change with the peak intensity of the laser pulse.

IV. CONCLUSION

We have presented a fully *ab-initio* and accurate study of the electron dynamics during the generation of below-threshold harmonics in H_2^+ molecular ions subject to intense near-infrared linearly and circularly polarized laser fields. The process has been analyzed at different laser wavelengths and internuclear separations in stretched H_2^+ molecules. Strong even harmonics are detected in the emitted radiation spectra. We have shown that this phenomenon has its origin in dynamic rupture of symmetry, when the electron is localized around one nucleus only for a substantial period of time exceeding half optical cycle. The symmetry in the distribution of the electron density is broken under the influence of the laser field when the electronic states with opposite inversion symmetry are both significantly populated. We emphasize the dynamic nature of this phenomenon: it takes place in the laser field despite the initial state ($1\sigma_g$) does have a definite parity, because the laser pulse itself does not satisfy the half-wave symmetry. In H_2^+, this situation is favored by

the charge resonance effect, where the $1\sigma_g$ and $1\sigma_u$ states are almost degenerate and have a strong dipole coupling at large internuclear separations. At smaller internuclear distances, possible one-photon resonance between these two states can also lead to generation of intense lines in the radiation spectra at the positions different from the normally expected odd integer multiples of the carrier frequency. We have performed a Floquet theoretical analysis based on the two-state approximation, which confirms the qualitative considerations given above. Possible experimental observation of even below-threshold harmonics can be done on H_2^+ prepared in excited vibrational states where the molecule spends a substantial amount of time in the stretched configuration or may be subject to dissociation under the influence of the laser field. We expect that even (as well as odd) below-threshold harmonic peaks in the HG spectra are not washed out by the molecular vibration since their positions in the spectra do not depend on R at large internuclear separations. We also note that this phenomenon is not specific for H_2^+ only. The charge resonance effect, which favors generation of even harmonics, may take place in any odd-charged homonuclear molecular ions. For the multielectron targets, our theoretical and computational approach can be extended with the help of the self-interaction free time-dependent density functional theory [36, 37].

ACKNOWLEDGMENTS

This work was partially supported by the Chemical Sciences, Geosciences and Biosciences Division of the Office of Basic Energy Sciences, US Department of Energy. We also would like to acknowledge the partial support from the Ministry of Science and Technology of Taiwan and National Taiwan University (Grant No. NTU-104R104021 and NTUERP-104R8700-2). D.A.T. acknowledges the partial support from St. Petersburg State University (Grant No. 11.38.654.2013). The images in Fig. 3 were generated using VisIt software [38]. VisIt is supported by the US Department of Energy with funding from the Advanced Simulation and Computing Program and the Scientific Discovery through Advanced Computing Program.

[1] M. Chini, X. Wang, Y. Cheng, H. Wang, Y. Wu, E. Cunningham, P.-C. Li, J. Heslar, D. A. Telnov, S. I. Chu, and Z. Chang, Nature Photonics **8**, 437 (2014).
[2] J.-C. Liu, M. C. Kohler, C. H. Keitel, and K. Z. Hatsagortsyan, Phys. Rev. A **84**, 063817 (2011).
[3] J. Henkel, T. Witting, D. Fabris, M. Lein, P. L. Knight, J. W. G. Tisch, and J. P. Marangos, Phys. Rev. A **87**, 043818 (2013).
[4] J. A. Hostetter, J. L. Tate, K. J. Schafer, and M. B. Gaarde, Phys. Rev. A **82**, 023401 (2010).
[5] N. H. Burnett, C. Kan, and P. B. Corkum, Phys. Rev. A **51**, R3418 (1995).
[6] M. Kakehata, H. Takada, H. Yumoto, and K. Miyazaki, Phys. Rev. A **55**, R861 (1997).
[7] P. B. Corkum, Phys. Rev. Lett. **71**, 1994 (1993).
[8] D. C. Yost, J. Schibli, Ye, J. L. Tate, J. Hostetter, M. B. Gaarde, and K. J. Schafer, Nature Phys. **5**, 815 (2009).
[9] H. Soifer, P. Botheron, D. Shafir, A. Diner, O. Raz, B. D. Bruner, Y. Mairesse, B. Pons, and N. Dudovich, Phys. Rev. Lett. **105**, 143904 (2010).
[10] H. Z. Jooya, D. A. Telnov, P.-C. Li, and S. I. Chu, Phys. Rev. A **91**, 063412 (2015).
[11] R. Kopold, W. Becker, and M. Kleber, Phys. Rev. A **58**, 4022 (1998).
[12] W.-H. Xiong, J.-W. Geng, J.-Y. Tang, L.-Y. Peng, and Q. Gong, Phys. Rev. Lett. **112**, 233001 (2014).
[13] K. Nasiri Avanaki, D. A. Telnov, and S.-I. Chu, Phys. Rev. A **90**, 033425 (2014).
[14] F. Martín, J. Fernández, T. Havermeier, L. Foucar, T. Weber, K. Kreidi, M. Schöffler, L. Schmidt, T. Jahnke, O. Jagutzki, A. Czasch, E. P. Benis, T. Osipov, A. L. Landers, A. Belkacem, M. H. Prior, H. Schmidt-Böcking, C. L. Cocke, and R. Dörner, Science **315**, 629 (2007).
[15] M. Kozlov, O. Kfir, A. Fleischer, A. Kaplan, T. Carmon, H. G. L. Schwefel, G. Bartal, and O. Cohen, New J. Phys. **14**, 063036 (2012).
[16] E. Frumker, C. T. Hebeisen, N. Kajumba, J. B. Bertrand, H. J. Wörner, M. Spanner, D. M. Villeneuve, A. Naumov, and P. B. Corkum, Phys. Rev. Lett. **109**, 113901 (2012).
[17] P. P. Corso, E. Fiordilino, G. Orlando, and F. Persico, J. Mod. Optics **54**, 1387 (2007).
[18] R. S. Mulliken, J. Chem. Phys. **7**, 20 (1939).
[19] D. A. Telnov and S.-I. Chu, Phys. Rev. A **76**, 043412 (2007).
[20] X. M. Tong and S. I. Chu, Chem. Phys. **217**, 119 (1997).
[21] D. A. Telnov, K. N. Avanaki, and S. I. Chu, Phys. Rev. A **90**, 043404 (2014).
[22] C. K. Chui, *An Introduction to Wavelets* (Academic Press, New York, 1992).
[23] X. Chu and S.-I. Chu, Phys. Rev. A **63**, 013414 (2001).
[24] X. M. Tong and S. I. Chu, Phys. Rev. A **61**, 021802 (2000).
[25] R. Bavli and H. Metiu, Phys. Rev. A **47**, 3299 (1993).
[26] O. E. Alon, V. Averbukh, and N. Moiseyev, Phys. Rev. Lett **80**, 3743 (1998).
[27] N. Moiseyev and M. Lein, J. Phys. Chem. A **107**, 7181 (2003).
[28] N. Moiseyev and F. Weinhold, Phys. Rev. Lett. **78**, 2100 (1997).
[29] D. A. Telnov and S. I. Chu, Phys. Rev. A **71**, 013408 (2005).
[30] D. A. Telnov, J. Wang, and S. I. Chu, Phys. Rev. A **52**, 3988 (1995).
[31] A. Fleischer, A. K. Gupta, and N. Moiseyev, International Journal of Quantum Chemistry **103**, 824 (2005).
[32] A. Fleischer and N. Moiseyev, Phys. Rev. A **74**, 053806 (2006).

[33] D. A. Telnov and S. I. Chu, J. Phys. B **28**, 2407 (1995).
[34] A. Fleischer and N. Moiseyev, Phys. Rev. A **72**, 032103 (2005).
[35] S. I. Chu and D. A. Telnov, Phys. Rep. **390**, 1 (2004).
[36] D. A. Telnov and S.-I. Chu, Phys. Rev. A **80**, 043412 (2009).
[37] J. Heslar, D. Telnov, and S.-I. Chu, Phys. Rev. A **83**, 043414 (2011).
[38] H. Childs, E. Brugger, B. Whitlock, J. Meredith, S. Ahern, D. Pugmire, K. Biagas, M. Miller, C. Harrison, G. H. Weber, H. Krishnan, T. Fogal, A. Sanderson, C. Garth, E. W. Bethel, D. Camp, O. Rübel, M. Durant, J. M. Favre, and P. Navrátil, in *High Performance Visualization–Enabling Extreme-Scale Scientific Insight* (2012) pp. 357–372.